Plasma Modification of Porous Structures for Formation of Composite Materials

Michelle L. Steen, Wendy C. Flory, Nathan E. Capps, and Ellen R. Fisher*

Department of Chemistry, Colorado State University, Fort Collins, Colorado 80523-1872

Received May 7, 2001
Revised Manuscript Received July 10, 2001

We have previously reported template synthesis of concentric composite micro- and nanostructured materials consisting of an outer tubule of one material surrounding inner tubes or fibers of different materials.[1] Composite nanostructures of metals, semiconductors, carbons, and polymers were prepared by several synthetic methodologies including electroless deposition, electropolymerization, carbonization, chemical vapor deposition (CVD), and sol−gel synthesis. Such materials are considered to have applications in microelectronics, chemical sensors, and electrochemical energy production.[2] Here, we report synthesis of three different composite materials utilizing plasma polymerization (PP) as one of the synthetic steps. First, template-synthesized micro- and nanostructured Au−polymer composites are presented, with the outer material produced via PP. With this system, we show for the first time that a high degree of granularity exists in the morphology of Au nanotubules produced via electroless deposition.

We also demonstrate the use of PP to produce two different types of microstructured materials, specifically integrated inorganic/polymer composite membranes and fibers as well as integrated polymer/polymer composite membranes. Particularly attractive aspects of PP for preparation of composites include production of conformal, pinhole-free materials with uniform thickness, availability of a wide range of chemistries and surface properties, and virtually unlimited monomer selection. Additional control of film chemistry is achievable via pulsed, downstream, and remote plasmas.[3] Here, we demonstrate the versatility of PP by producing integrated composite membranes where the surface coating is tailored for a specific chemistry. These novel materials have potential applications as replacements for spun-glass filters, air-vent filters, and biomolecule separations.

Gold tubes (from 200 nm to 2 μm) were prepared from template track-etched polyester (PET) membranes using electroless deposition as described previously.[4,5] The membrane is removed with hexafluoro-2-propanol to reveal free-standing Au structures.[1] Figure 1A shows a field-emission scanning electron micrograph (FE-SEM) of Au tubes prepared from 200-nm template membranes. This image displays a level of porosity that has not previously been reported for Au tubes prepared by electroless deposition. This type of granularity has, however, been reported for metal nanotubes produced via electrochemical deposition.[6] In both processes, Au particles are deposited at metal complexation sites on the pore walls and membrane surfaces.[7] The nanoscopic holes (≈50−100 nm diameter) in the structure of the Au tubes shown in Figure 1A could be the result of a limited number of complexation sites on the pore walls. Alternatively, formation of grain boundaries, defects, or vacancies in the metal could also explain the incomplete congealing of the growing material. Previously reported SEM images of similar Au structures taken with lower resolution instruments (only ≈50 nm) did not contain enough detail to completely discern the morphology shown clearly in Figure 1A.[7]

To form a Au/polymer composite, an outer tubule of the electronically conductive polymer polypyrrole was deposited on the Au tubules through pulsed PP of pyrrole (5% duty cycle, 200-W peak applied rf power, pressure = 150 mTorr)[8] using our inductively coupled tubular glass plasma reactor described in detail previously.[9] Figure 1B shows a high-magnification SEM of 1-μm Au tubules prior to plasma deposition and Figure 1C shows the same tubules after deposition. It is clear from Figure 1C that the polymer coating has clearly covered the entire length of the tubules, that the ends are capped with the coating, and that none of the underlying Au is exposed. Given the relatively high deposition rate (>1000 Å/min), it is unlikely that the polymer layer fills the interior of the tubule prior to capping.

FTIR spectra of the polymer layer indicate characteristic pyrrole absorbances such as N−H stretching at 3400 cm^{-1}, the =C−H in-plane deformation at 1037−1096 cm^{-1} from aromatic ring breathing of pyrrole and the −C−H out-of-plane deformation at 740 cm^{-1}. Absorption peaks at 2219 cm^{-1} (C≡N stretching) and 2900 cm^{-1} (aliphatic C−H stretching) indicate partial ring opening of pyrrole during PP. Although thin film materials have been produced via CW PP of pyrrole,[10,11] our films retain more of the monomer structure because of the milder pulsed conditions. Indeed, we have shown

* To whom correspondence should be addressed. E-mail: erfisher@lamar.colostate.edu.

(1) Cepak, V. M.; Hulteen, J. C.; Che, G.; Jirage, K. B.; Lakshmi, B. B.; Fisher, E. R.; Martin, C. R. *J. Mater. Res.* **1998**, *13*, 3070. Cepak, V. M.; Hulteen, J. C.; Che, G.; Jirage, K. B.; Lakshmi, B. B.; Fisher, E. R.; Martin, C. R. *Chem. Mater.* **1997**, *9*, 1065.

(2) Che, G.; Miller, S. A.; Fisher, E. R.; Martin, C. R. *Anal. Chem.* **1999**, *71*, 3187.

(3) We and others have demonstrated this previously with a variety of materials. See Savage, C. R.; Timmons, R. B. *Chem. Mater.* **1991**, *3*, 575. McCurdy, P. R.; Truitt, J. M.; Fisher, E. R. *J. Electrochem. Soc.* **1998**, *145*, 3271. Butoi, C. I.; Mackie, N. M.; Barnd, J. E.; Fisher, E. R.; Gamble, L. J.; Castner, D. G. *Chem. Mater.* **1999**, *11*, 862.

(4) Nishizawa, M.; Menon, V. P.; Martin, C. R. *Science* **1995**, *168*, 700.

(5) Menon, V. P.; Martin, C. R. *Anal. Chem.* **1995**, *67*, 1920.

(6) Schonenberger, C.; van der Zande, B. M. I.; Fokkink, L. G. J.; Henny, M.; Schmid, C.; Krueger, M.; Bachtold, A.; Huber, R.; Birk, H.; Stauffer, U. *J. Phys. Chem. B* **1997**, *101*, 5497.

(7) Hulteen, J. C.; Martin, J. C. *J. Mater. Chem.* **1997**, *7*, 1075.

(8) Duty cycle is defined as the ratio of on time to total cycle time multiplied by 100.

(9) Bogart, K. H. A.; Dalleska, N. F.; Bogart, G. R.; Fisher, E. R. *J. Vac. Sci. Technol. A* **1995**, *13*, 476.

(10) Lee, K. P.; Park, S. Y.; Kim, N.; Song, S. K. *Mol. Cryst. Liq. Cryst.* **1993**, *224*, 53.

(11) Cruz, G. J.; Morales, J.; Olayo, R. *Thin Solid Films* **1999**, *342*, 119.

10.1021/cm010452q CCC: $20.00
Published on Web 08/30/2001

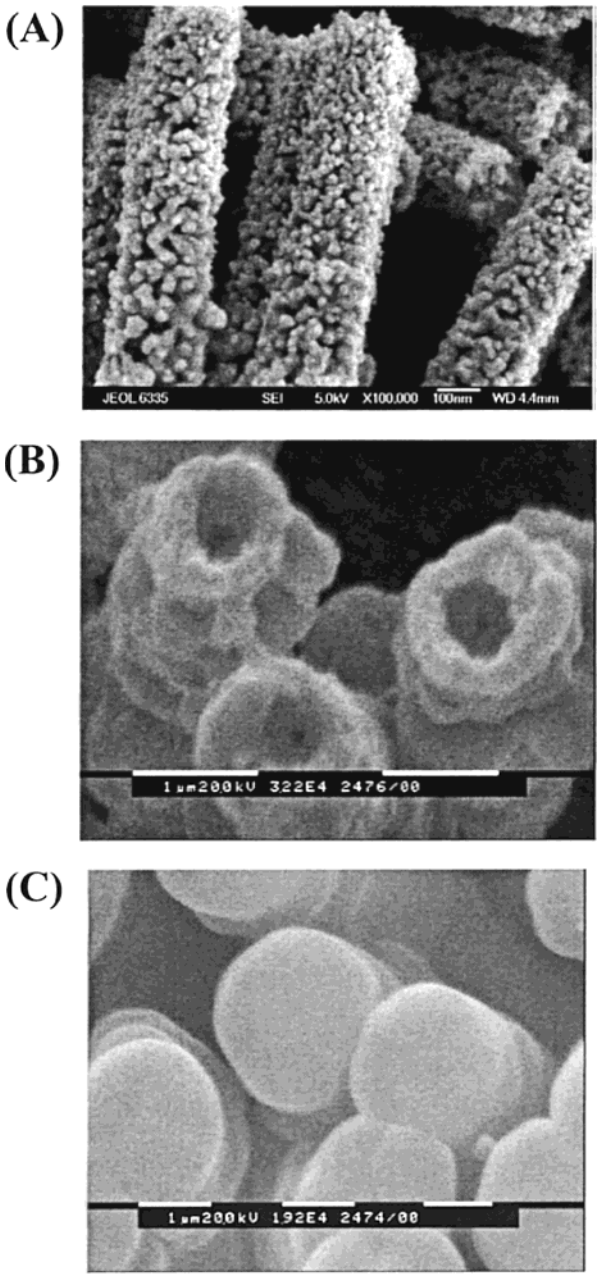

Figure 1. (A) A high-resolution (10^5 X) FE-SEM of Au tubules grown in 200-nm membranes after dissolution of the template. Note the high porosity over the entire surface of the tubules, which is likely caused by the granularity of the metal. (B) SEM image of Au tubules grown in 1-μm membranes after dissolution of the template. (C) SEM image of the 1-μm Au tubules with an ca. 1-μm-thick conformal coating of polypyrrole deposited using a pulsed pyrrole plasma (30-min deposition).

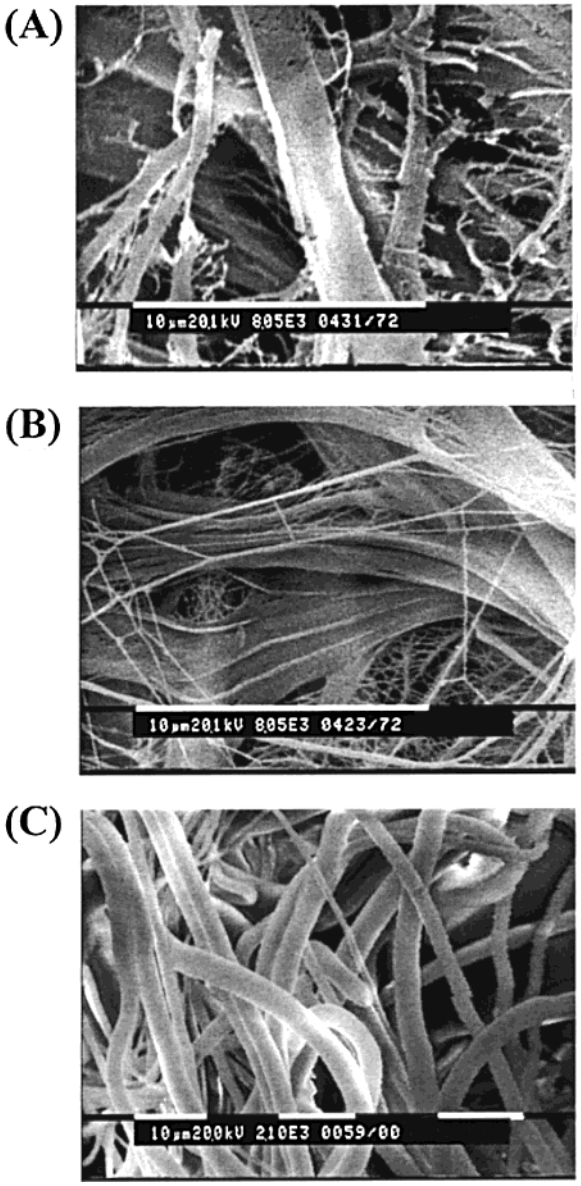

Figure 2. (A) SEM image of an untreated microporous polyethylene membrane. (B) The same microporous PE membrane with ≈800 Å of SiO_2 deposited from a 25-W CW HMDSO:O_2 (1:9) plasma (10 min, 100 mTorr). The membrane was placed in the membrane holder, 9 cm downstream from the coil region of the plasma. (C) Nonwoven PET fibers coated with ≈800 Å of SiO_2 using the same conditions as in (B).

that pulsed plasmas afford greater control over film chemistry in PP, including retention of aromaticity.[12] Preliminary results from electrochemical characterization of the materials shown in Figure 1C indicate our plasma-polymerized polypyrrole films are indeed conducting. The two most important results in this system are (1) that we can achieve smooth, pinhole-free, conformal, and complete coating of the porous Au nanostructures (from 200 nm to 2 μm in diameter) and (2) we can tailor the polymeric film chemistry and thickness as desired. Indeed, we have also demonstrated this capability with both insulating and conductive polymer coatings, such as polystyrene-like materials from benzene plasmas.[13]

Figure 2 shows SEM images of our second system with ≈100-μm-thick microporous symmetric polyethylene (PE) membranes, Figure 2A, and nonwoven PET fibers as host materials.[14] Here, an inorganic coating is applied to the polymer substrates using the same plasma reactor as above with a CW hexamethyldisilox-

(12) (a) Leich, M. A.; Mackie, N. M.; Williams, K. L.; Fisher, E. R. *Macromolecules* **1998**, *31*, 7618. (b) Mackie, N. M.; Castner, D. G.; Fisher, E. R. *Langmuir* **1998**, *14*, 1227.

(13) Details of this polymerization, including extensive surface analysis (FTIR, XPS, SIMS) of the deposited materials and demonstration of their polystyrene-like nature can be found in ref 12b.

(14) Both the PE and PET materials have 1−10 μm pores or voids throughout the thickness.

ane (HMDSO)/O_2 (1:9) plasma (rf power = 25 W; pressure = 100 mTorr) which deposits SiO_x films.[15] To optimize modification of the entire cross section of these porous materials, a special membrane holder orients these materials perpendicular to gas flow and forces the plasma to penetrate through the membrane.[16,17] Figure 2B demonstrates we have conformal coverage of the PE membrane, where the pore size is not significantly altered and there is no sign of pore filling. Furthermore, we have shown using environmental SEM[18] that complete modification of the membrane cross section is achieved with our experimental configuration. Film growth on the PE membrane includes formation of thin, continuous fibers that span the entrance of the pore cavities. Although these fibers are not present in the SEM of the nonwoven PET fibers, energy-dispersive spectroscopy (EDS) did detect the presence of silicon on the plasma-treated PE and PET, which was not observed with the untreated materials.

Chemical analyses utilizing X-ray photoelectron spectroscopy (XPS), variable angle spectroscopic ellipsometry (VASE), and FTIR verified the deposited material is SiO_2. The high-resolution O_{1s} XPS spectrum confirmed that the deposited material consists primarily of SiO_x groups with stoichiometric O/Si atomic ratios of 2.6−3.0 for the plasma-treated polymers. VASE analysis using a SiO_2 model[19] also confirms that the plasma-deposited film is SiO_2. The model provides film thickness, 804 ± 33 Å, and refractive index (1.4422−1.4702 for λ = 200−700 nm), agreeing with literature values for SiO_2.[20] The FTIR spectrum displays absorption bands at ≈1070 and ≈820 cm^{-1}, corresponding to SiO stretching and bending modes, respectively. Additional absorbance bands at ≈924 and ≈3400 cm^{-1} are attributable to Si−OH vibrations.

Although silanol incorporation is undesirable in many microelectronics applications, it is a criterion for filter applications needing hydrophilic surfaces. Our SiO_2/polymer composites wet immediately and completely with water. In contrast, the untreated polymers are naturally hydrophobic with contact angles of 105.2 ± 6.5° (PE) and 132.9 ± 3.5° (PET). More importantly, both sides of the treated materials were wettable, further evidence that our process modifies the entire cross section[21] and that the inorganic layer is integrated throughout the porous structure.[22,23] This maintains homogeneous porosity throughout the modified materials, such that permeation characteristics are essentially unchanged.[18] Most composite membranes (a dense top layer with a microporous sublayer) have dissimilar permeation rates across the membrane.[24] Plasma processes have been employed to prepare such composite membranes by deposition of a second polymer onto a homogeneous membrane,[25] to deposit a skin layer onto an asymmetric membrane support,[26] or to chemically modify the existing skin layer to produce composite membranes.[27] In each of these examples only one membrane surface was intentionally modified to produce a selective layer with a specific chemistry. In contrast, our synthetic strategy produces membranes with tailored surface properties, without significantly altering the porosity. To our knowledge, this is the first report of such integrated inorganic/polymer composite materials.

The third system, microstructured polymer/polymer integrated membranes uses 150-μm-thick asymmetric polysulfone (PSf) membranes, Figure 3A, as the host material. These membranes have an average pore size of 1.2 μm on the open side, minimum pore diameters of ≈0.133 μm on the tight side, and nominal bubble points of 57 ± 3 psi.[16] Figure 3B shows a PSf membrane coated with ≈80 Å of a fluorocarbon polymer using pulsed PP of hexafluoropropylene oxide (HFPO) (same reactor, 16% duty cycle, 300-W peak applied rf power, pressure of 230 mTorr). Extensive surface analyses revealed these materials are highly ordered CF_2 chains, oriented perpendicular to the underlying substrate and terminated at the surface with CF_3.[28] Contact angle measurements made on both sides of this integrated composite membrane indicate an increase in the hydrophobicity of the material, from ≈90° to ≈110°, again indicating penetration of the plasma through the porous host. Cross-section SEM analysis of the treated membrane is nearly identical to that in Figure 3C. Moreover, comparison to Figure 3A shows film deposition has not adversely affected the porosity of the membrane. This is confirmed by bubble point measurements, which indicate no significant change in pore size. In contrast, hydrophobic modification with a CW CHF_3 plasma, forming an amorphous fluorocarbon polymer,[29] did not result in conformal coverage of the membrane structure. From the cross-sectional images in Figure 3C,D, it is clear the deposited material has decreased pore diameter, thereby losing the membrane structure.[30] The primary reason for the differences observed between the

(15) Steen, M. L.; Fisher, E. R. *J. Electrochem. Soc.*, submitted for publication.

(16) Steen, M. L.; Hymas, L.; Havey, E. D.; Capps, N. E.; Fisher, E. R. *J. Membr. Sci.* **2001**, *188*, 97−114.

(17) Treating multiple membranes in the holder simultaneously explicitly shows that the interior surfaces of a stacked assembly are completely modified, such that penetration around the edges cannot explain the results. Depth of penetration is estimated at ∼150−300 μm (i.e., two membranes). While the mechanism for plasma penetration is not fully understood, our previous work has shown that penetration is related to both membrane material (composition) and structure (degree of asymmetry). See Steen, M. L.; Butoi, C. I.; Fisher, E. R. *Langmuir*, submitted for publication, as well as refs 16 and 18.

(18) Steen, M. L.; Jordan, A. C.; Fisher, E. R. *J. Membr. Sci.*, submitted for publication.

(19) Woolam, J. A.; Snyder, P. G.; Rost, M. C. *Thin Solid Films* **1988**, *166*, 317. Logothetidis, S.; Boultadakis, S. *J. Appl. Phys.* **1995**, *78*, 5362.

(20) Adams, A. C. In *Plasma Deposited Thin Films*; Mort, J., Jansen, F., Eds.; Chemical Rubber: Boca Raton, FL, 1986.

(21) We have seen this type of extensive penetration previously with plasma modification of ultrafiltration and microporous membranes. See ref 16.

(22) Penetration of nonwoven fibers by polymer-forming plasmas was not observed by Yasuda and co-workers. Yasuda, T.; Okuono, T.; Miyama, M.; Yasuda, H. *J. Polym. Sci. A: Polym. Chem.* **1994**, *32*, 1829.

(23) Again, this has been verified with the multiple membrane experiments described above and in ref 16 as well as with environmental SEM data. See also ref 18.

(24) Mulder, M. *Basic Principles of Membrane Technology*; Kluwer Academic Press: Boston, 1996; p 13.

(25) Lin, X.; Chen, J.; Xu, J. *J. Membr. Sci.* **1994**, *90*, 81. Inagaki, N.; Tasaka, S.; Murata, T. *J. Appl. Polym. Sci.* **1992**, *38*, 1869.

(26) Hopkins, J.; Badyal, J. P. S. *Langmuir* **1996**, *12*, 4205.

(27) Hopkins, J.; Badyal, J. P. S *Langmuir* **1996**, *12*, 3666.

(28) Butoi, C. I.; Mackie, N. M.; Gamble, L. J.; Castner, D. G.; Miller, A. E.; Barnd, J. E.; Fisher, E. R. *Chem. Mater.* **2000**, *12*, 2014.

(29) Capps, N. E.; Mackie, N. M.; Fisher, E. R. *J. Appl. Phys.* **1998**, *84*, 4736.

(30) This has been observed previously for high deposition rate systems. Onishi, M.; Shimura, K.; Seita, Y.; Yamashita, S.; Takahashi, A.; Masuoka, T. *Radiat. Phys. Chem.* **1992**, *39*, 569.

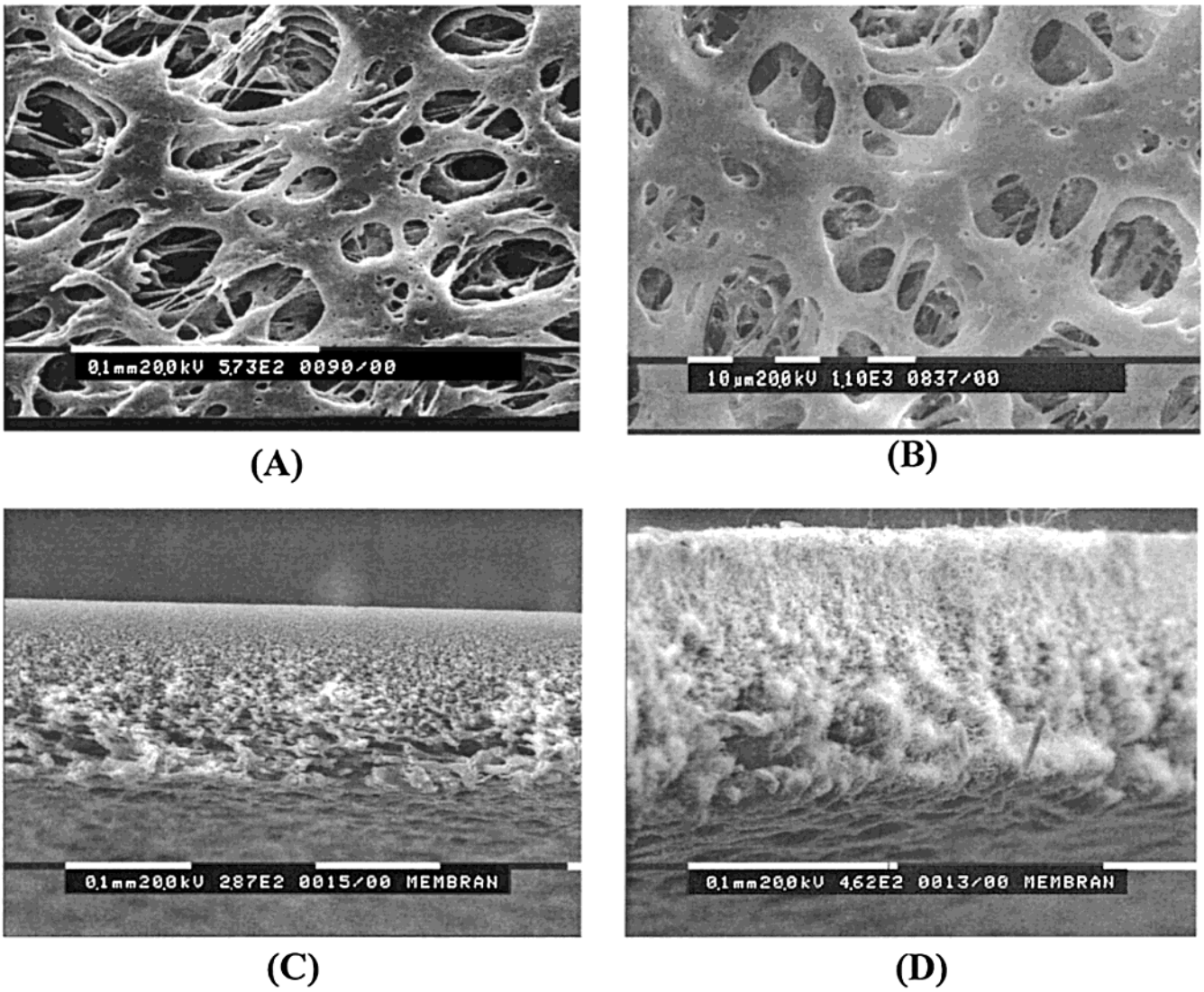

Figure 3. (A) SEM image of the surface of an untreated microporous polysulfone membrane. (B) The same PSf membrane ≈80 Å of a conformal ordered CF_2-rich fluorocarbon polymer deposited from a pulsed HFPO plasma (16% duty cycle, 300-W peak applied rf power, 10 min, 233 mTorr). (C) SEM image of the cross section of an untreated PSf membrane. (D) Cross-sectional SEM image of the same membrane treated with a 80-W CW CHF_3 plasma (10 min, 150 mTorr). Note that deposition in this system drastically alters the underlying membrane structure. All treatments were performed using the membrane holder, placed 8−9 cm downstream from the coil region of the plasma.

HFPO and CHF_3 systems is the greater control over film chemistry and deposition rate realized by pulsed PP. The HFPO system does, however, demonstrate the range of materials chemistry and surface properties possible for these integrated membrane systems. Thus, the synthetic strategies utilized here for these model systems point to numerous possibilities for other novel composite materials. We are currently exploring some of these possibilities along with potential applications for all three composite materials presented here.

Acknowledgment. This work was supported by the National Science Foundation and the Membrane Applied Science and Technology Center in Boulder, CO.

CM010452Q